HHS Public Access

Author manuscript

Methods. Author manuscript; available in PMC 2019 January 03.

Published in final edited form as:

Methods. 2016 March 01; 96: 46–58. doi:10.1016/j.ymeth.2015.08.024.

A high-content imaging-based screening pipeline for the systematic identification of anti-progeroid compounds

Nard Kubben[a], **Kyle R. Brimacombe**[b], **Megan Donegan**[a], **Zhuyin Li**[b,1], and **Tom Misteli**[a,*]

[a]National Cancer Institute, National Institutes of Health, Bethesda, MD 20892, USA

[b]National Center for Advancing Translational Sciences, National Institutes of Health, Rockville, MD 20850, USA

Abstract

Hutchinson–Gilford Progeria Syndrome (HGPS) is an early onset lethal premature aging disorder caused by constitutive production of progerin, a mutant form of the nuclear architectural protein lamin A. The presence of progerin causes extensive morphological, epigenetic and DNA damage related nuclear defects that ultimately disrupt tissue and organismal functions. Hypothesis-driven approaches focused on HGPS affected pathways have been used in attempts to identify druggable targets with anti-progeroid effects. Here, we report an unbiased discovery approach to HGPS by implementation of a high-throughput, high-content imaging based screening method that enables systematic identification of small molecules that prevent the formation of multiple progerin-induced aging defects. Screening a library of 2816 FDA approved drugs, we identified retinoids as a novel class of compounds that reverses aging defects in HGPS patient skin fibroblasts. These findings establish a novel approach to anti-progeroid drug discovery.

Keywords

HGPS; Progerin; Retinoids; FDA-approved compounds; High-throughput screening; High-content imaging

1. Introduction

Hutchinson–Gilford Progeria Syndrome is a premature aging disease in which a de-novo point mutation in exon 11 of the *LMNA* gene, encoding for the nuclear architectural lamin A and C proteins, causes early onset of metabolic, skin, bone and cardiovascular anomalies that become ultimately lethal before patients reach adulthood [14]. These clinical

*Corresponding author. mistelit@mail.nih.gov (T. Misteli).

[1]Current address: Lead Discovery and Optimization, Bristol-Meyers Squibb, 5 Research Parkway, Wallingford, CT 06492, USA.

Author contributions

NK and TM designed the study; NK performed all experiments, except for the primary compound screen, which was performed by KB and ZL, and real-time PCR analysis which was performed by MD; NK and TM wrote the manuscript. All authors read and approved the manuscript.

Conflict of interest

The authors declare no conflicts of interest.

Appendix A. Supplementary data

Supplementary data associated with this article can be found, in the online version, at http://dx.doi.org/10.1016/j.ymeth.2015.08.024.

manifestations are caused by the activation of an alternative cryptic splice site which results in the expression of progerin, a lamin A mutant that lacks 50 amino acids and as a result remains permanently farnesylated at its C-terminal CAAX motif [4]. Progerin acts in a dominant negative fashion, and diminishes the nucleus' architectural integrity, as well as compromises heterochromatin maintenance, DNA repair, and numerous other cellular processes through yet unknown mechanisms [16].

Experimental approaches to identify druggable targets that counteract progerin-induced aging defects have mainly used a bottom-up strategy, in which pathways affected by progerin are studied one at a time and the gained molecular mechanistic insight is subsequently used for drug development to ameliorate specific pathways compromised in HGPS. Such experimental approaches have led to the identification of drugs with favorable nuclear structural effects, such as farnesyl transferase inhibitors (FTIs) that prevent accumulation of farnesylated progerin at the nuclear lamina [48,53]; heterochromatin promoting compounds, like the SIRT1-activating compound resveratrol [3,23,51]; DNA damage reducing antioxidants such as N-acetyl cysteine or remodelin, an inhibitor of the acetyl transferase NAT10 [22,39]; anti-inflammatory drugs such as the NFkB inhibitor salicylate [31]; and mitochondrial integrity improving compounds such as pyrophosphate [49]. While FTIs have been used in clinical trials with partial effects [15], none of the others compounds have reached the clinic for treatment of HGPS.

The success of these bottom-up approaches is highly dependent upon the identification of well-defined disease-driving defects, which is challenging in the case of HGPS, given that pleiotropic cellular phenotypes make it difficult to determine whether progerin impaired pathways drive the HGPS phenotype or are mere bystanders. A further complication in HGPS drug discovery is the challenge of using primary HGPS patient cells to identify druggable targets, because HGPS patient cells are restricted in their *in vitro* growth, show considerable variability in phenotype and response between patients, and many of the progerin-induced aging defects appear to be stochastic in nature [20,42].

To overcome these limitations, we describe here an unbiased top-down screening approach to HGPS drug discovery. The method is based on the quantitative assessment of the ability of small compounds to prevent the formation of structural, epigenetic, and DNA damage related nuclear defects triggered by the disease-causing progerin protein. We report the development of a doxycycline-inducible progerin wildtype fibroblast cell line, which allows for systematic identification of compounds with anti-progeroid effects in a high-content and high-throughput fashion. As proof-of-principle for the validity and usefulness of this novel discovery tool we performed a screen of FDA-approved compounds and identified retinoids as a novel class of drugs that can be used to restore aging defects in HGPS patient cells.

2. Materials and methods

2.1. Cloning and generation of cell lines

GFP-lamin A, GFP-progerin, and GFP-progerin C661S doxycycline inducible dermal fibroblast cell lines were generated through sub-cloning from GFP-lamin A and GFP-progerin containing pBabepuro plasmids as previously described [44] into the pENTR1A-

no-ccDB plasmid (Addgene, #17398). Quickchange II XL site directed muta-genesis was used according to manufacturer's instructions (Agilent) to mutate the cysteine of the carboxy terminal CAAX farnesylation motif into a serine, thereby generating pENTR1A-GFP-Progerin C661S. Gateway-mediated LR recombination (Invitrogen) was applied to transfer all three GFP-lamin constructs into the pLentiCMVTRE3G-Neo plasmid (Addgene, #w813–1). Next hTert immortalized human dermal fibroblasts [44] were infected with lentivirus generated as previously described [18] from the doxycycline inducible pLentiCMVTRE3G-Neo-GFP-lamin constructs and the constitutively tetracycline repressor A3 mutant expressing pLentiCMVrtTA3-Hygro plasmid (Addgene, #26730). After antibiotic selection (Hygromycin and G418 both at 200 μg/ml) individual clones were picked based on the criteria of having induced GFP-lamin levels equal to endogenous lamin A expression after 4 days of doxycycline induction as assessed by western blot analysis. Two clones were picked for each of the GFP-tagged lamin constructs. Experiments comparing the effect of induced GFP-lamin A, GFP-progerin and GFP-progerin C661S were comparable between pairs of clones for the same lamin construct and are represented as the average of both clones. The inducible GFP-progerin P1 clone was used for high-throughput drug screening.

2.2. Tissue culture and cell treatments

We obtained primary dermal fibroblasts cells from HGPS patients (Coriell Cell repository (CCR) #AG01972) and age-matched healthy controls (American Type Culture Collection #CRL-1474; CCR #GM00038). All experiments in HGPS patient cells were performed in primary AG01972 cells, except for hTert immortalized HGPS (#AG01972) patient cells [44] that were used for studying the effect of retinoid drugs on A-type lamin protein and mRNA expression levels. All primary cell lines were used at passage doublings 16 to 24 and grown under similar conditions as hTert immortalized HGPS patient fibroblasts and GFP-lamin inducible cell lines in Minimum Essential Medium (Life Technologies) supplemented with 15% FBS, 2 mM L-Glutamine, 1 mM sodium pyruvate, non-essential amino acids, and 100 U/ml penicillin and 100 μg/ml streptomycin at 37 °C in 5% CO_2.

Cell treatments were performed for 4 days in GFP-lamin inducible cell lines and for 8 days in HGPS patient and control cells at the following concentrations, unless indicated otherwise in the respective figure legends: farnesyl transferase inhibitor L-744,832 (5 μM; Sigma, #L7287), isotretinoin (10 μM; Sigma, #1353500–200MG), tamibarotene (10 μM; Sigma, #T3205–5MG) and tazarotene (10 μM; Sigma, T7080–10MG). FDA-approved drugs used in the primary and validation screen were obtained from an in-house library of the National Center for Advancing Translational Sciences (NCATS, Rockville, USA). All compounds were dissolved in DMSO and final concentrations of DMSO did not exceed 0.25%. For GFP-lamin inducible cell lines, cells were plated in 384-well plates in the presence of compounds and left without medium change for the duration of the experiment (4 days). For HGPS patient and control cells, cell were grown for four days in 6-well plates, with replacement of compounds and medium every other day, prior to plating into 384 well plates in the presence of compounds that were replaced once more midway through the experiment (after 2 days).

2.3. High-throughput screening assay

Primary screening of this assay was performed using an NCATS in-house library (NCGC Pharmaceutical Collection, NPC) [17] of 2816 FDA-approved compounds, for which the effect on the induction of GFP-progerin and formation of lamin B1 and γH2AX nuclear defects in P1 GFP-progerin inducible cells was tested at four concentrations (1, 3, 10 and 29 μM) in 384-well PE-Cell Carrier imaging plates (Perkin Elmer). 400 P1 cells suspended in 30 μl growth medium (see above), supplemented with 1 μg/ml doxycycline for induction of GFP-progerin expression, were seeded per well using a Multidrop Combi Reagent dispenser (ThermoFisher Scientific). 86 nL of concentrated DMSO compound stocks were transferred to the wells, following cell attachment using a 384-well pintool. Compound treatments were split over four independently processed 384-well plates, one for each final concentration (1, 3, 10 or 29 μM), with no experimental repeats. Non compound treated doxycycline GFP-progerin induced cells served as a negative control. P1 cells in which GFP-progerin remained uninduced, or in which GFP-progerin was induced in the presence of 5 μM farnesyl transferase inhibitorL-744,832 served as positive controls. After initial plating, the cells were incubated for 96 h at 37 °C and 5% CO_2, after which they were fixed by the addition of paraformaldehyde to a final concentration of 4% (10 min), permeabilized (PBS/0.5% triton-X 100; 10 min), and washed once with PBS/0.05% Tween-20 using a BioTek Microplate washer. All further washes were performed using the BioTek Microplate washer using plate optimized height and volume settings. Immunofluorescence staining was performed by a 1 h incubation in block buffer (PBS/0.05% Tween-20, 5% bovine serum albumin) diluted primary antibodies (goat-anti-lamin B1, 1:500, SantaCruz Sc-6217; mouse-anti-γH2AX, 1:1000, Millipore #05–636), followed by two washes in PBS/0.5% Tween-20, one wash in PBS/0.05% Tween-20, a 1 h incubation with fluorescent labeled secondary antibodies (Alexa Fluor Donkey-anti-Goat 647, Invitrogen #A21447; Donkey-anti-Mouse 568, 1:500 Invitrogen #A10037) in the presence of 5 μg/ml DAPI, two washes in PBS/0.5% Tween-20, one wash in PBS/0.05% Tween-20, and final storage of the plates in PBS/0.05% Tween-20 at 4 °C. For validation experiments the following antibodies were used for immunofluorescence staining in 384-well plates: mouse-anti-Progerin (1:10, Alexis Biochemicals ALX-804–662), rabbit-anti-LAP2 (1:200; Santa-Cruz Sc-28541), mouse-anti-HP1γ (1:4000, ChemiconMAB3450), rabbit-anti-trimethylated histone 3 lysine 27 rabbit polyclonal (H3-K27–3M; 1:500, Upstate #07–449) and rabbit-anti-53BP1 (1:2000, Novus NB100–304).

2.4. High-throughput immunofluorescence microscopy and automated image analysis

Using an Opera high-throughput spinning-disk confocal microscopy system (Perkin Elmer), cells were imaged in a single optimal focal plane with a 20× water immersion objective in three independent acquisitions (405/640 nm, 488 nm and 568 nm excitation lasers). Captured images were analyzed using custom-developed Acapella Software (Perkin Elmer) image analysis algorithms. After initial nuclear segmentation based on DAPI staining, including a minimal and maximal nuclear area threshold, the overall nuclear intensity was determined for GFP-progerin, lamin B1, and in validation experiments, for LAP2, HP1γ and histone 3 tri-methylated lysine 27 (H3-K27–3M). For γH2AX, and in validation experiments for 53BP1, individual nuclear foci were detected using a contrast-based algorithm [40] that combines the number, area, and brightness of detected foci into one

integrated parameter per cell. All IF quantifications of γH2AX and 53BP1 as displayed in the figures or referred to in the text are based on this nuclear foci detection algorithm. Minimally 300 cells were imaged for each condition in each experiment and parameters were calculated as averages of the total cell population. Using the CellHTS2 package [34,35], normalized *Z*-scores for GFP-progerin, lamin B1 nuclear intensity and γH2AX integrated foci intensity were calculated. Based on positive (GFP-progerin not induced) and negative controls (GFP-progerin induced), *Z′*-score for the assays parameters were 0.17 for lamin B1, 0.34 for γH2AX, and 0.83 for progerin.

2.5. Screening data analysis

Each tested concentration of the NPC library compounds was analyzed independently, and compounds were considered candidates if minimally 2 of the 4 tested concentrations either significantly lowered induced GFP-progerin (*Z*-score > 4.00) or prevented the formation of nuclear defects in lamin B1 (*Z*-score < −1.75) or γH2AX (*Z*-score > 1.75), without cytotoxic effects as defined by cell numbers above 50% of the negative control. Initial candidates that prevented the formation in lamin B1 defects were further selected based on their ability to reduce γH2AX defects, and vice versa those that reduced γH2AX were cross-compared to their effect on lamin B1, by combining the effects on lamin B1 and γH2AX with equal weights into a single parameter and applying a cut-off *Z*-score < −2.00. For validation of candidate compounds, primary HGPS patient cells were grown for 4 days in 6-well plates in the presence of candidate compounds at their most optimal concentration as determined in the primary screen (10 μM, unless mentioned otherwise in figure legends), and plated at a density of 2000 cells per 50 μml growth medium in 384 well-plates. After four days of growth, cells were fixed and stained as described above for progerin, lamin B1, LAP2, HP1γ, H3-K27–3M, γH2AX, and 53BP1.

2.6. Western blotting

For western blot analysis cells were trypsinized, and equal number of cells were dissolved in SDS–PAGE Laemmli sample buffer, and subsequently denatured for 5 min at 95 °C. Equal amounts of protein extract were loaded onto NuPage Novex Bis-Tris 4–20% gradient gels (Lifesciences), blotted on immobilon-PVDF membrane (Millipore), blocked for 1 h in 5% milk powder/TBS-T (20 mM Tris–HCl pH 7.5, 150 mM NaCl and 0.1% Tween-20). Blocked membranes were incubated overnight at 4 °C with block buffer diluted goat-anti-lamin A/C (SantaCruz, Sc-6215) or mouse-anti-βActin (Sigma, A2228) primary antibody as per manufacturer's instructions. After incubation with appropriate HRP-conjugated secondary antibodies (Amersham), protein detection was performed with the ECL western blotting detection system (Amersham) and recorded on a Biorad ChemiDoc imaging system. The intensity of signals was quantified using Biorad Image Lab software and statistically analyzed with a Student's *t*-test.

2.7. Quantitative analysis of gene expression

RNA samples were prepared as previously described [18] and mRNA expression levels of lamin A, progerin and lamin C were determined using the following primers: 5′-GGTGCGCTCAGT GACTGT-3′ & 5′-GCTGCTGCAGTGGGAGC-3′ (lamin A); 5′-GCGTCAGGAGCCCTGAGC-3′ & 5′-GCTGCTGCAGTGGGAGC-3′ (progerin); 5′-

ACGGCTCTCATCAACTCCAC-3′ & 5′ -GCGGCGGCTACCACTCAC-3′ (lamin C); 5′ -CTGTTGCTGTAGCCAAATTCGT-3′ & 5′ -ACCCACTCCTC CACCTTTGA-3′ (housekeeping gene GAPDH), using 40 amplification cycles (95 °C 20 s–56 °C 30 s) on a Biorad CFX96 Real-Time PCR machine.

3. Results

3.1. Development of GFP-progerin inducible wildtype skin fibroblasts

We set out to develop a high-throughput method for the systematic and unbiased identification of compounds that affect cellular HGPS driver pathways to overcome limitations of currently used low-throughput, hypothesis-driven assays. In order to study the effects of compounds on the formation of primary HGPS defects, as opposed to secondary defects already present in cells chronically expressing progerin, we generated a progerin inducible cell-based system. To this end we genetically modified wildtype hTERT immortalized human skin fibroblasts to express GFP-progerin under the control of a doxycycline inducible promoter (Fig. 1A). In the absence of doxycycline, GFP-progerin levels were close to the detection limit of immunofluorescence and western blot analysis (Fig. 1B and C), but following the addition of low amounts of doxycycline over several days, GFP-progerin levels were induced steadily and without sudden expression bursts, and reached moderate protein expression levels comparable to endogenous lamin A within 4 days (Fig. 1C). GFP-progerin localized correctly to the nuclear lamina (Fig. 1B).

Cell-based high-throughput screening assays for dominant negative disease models require the induction of strong phenotypes that are specific for the disease-causing mutant protein. To establish specificity of the effects caused by GFP-progerin, we compared GFP-progerin effects to analogous wild-type fibroblasts expressing wild-type GFP-lamin A or GFP-progerin-C661S (Fig. 1A). The C661S point mutation serves as a negative control since it affects the cysteine of the progerin C-terminal CAAX motif, thereby rendering it defective for posttranslational farnesylation [52]. This redirects the pathogenic accumulation of permanently farnesylated lipophylic progerin at the nuclear periphery into the less harmful accumulation of intranuclear non-farnesylated progerin aggregates [52]. Both GFP-lamin A and GFP-progerin-C661S were induced to protein levels comparable to GFP-progerin in the established inducible wildtype fibroblasts cell lines ($p < 0.05$; Fig. 1C), and localized as expected to the nuclear lamina and intranuclear foci, respectively (Fig. 1B).

3.2. Phenotype characterization of inducible GFP-progerin cell system

To determine the suitability of inducible GFP-progerin cells for high-throughput screening purposes, time course experiments were performed to assess the effect of GFP-progerin and its controls on several previous reported HGPS cellular defects including reduced levels of the structural nuclear proteins lamin B1 and LAP2, heterochromatin promoting HP1γ and tri-methylated lysine 27 of histone 27 (H3-K27–3M) [43], and activation of DNA damage signaling as measured by increased formation of 53BP1 and Serine 139 phosphorylated H2AX (γH2AX) foci formation [26]. Upon doxycycline addition, steadily increasing GFP-progerin protein levels were already detectable at 12 h post induction. Concomitantly, lamin B1, LAP2, HP1γ and H3-K27–3M levels decreased correspondingly, all reaching significant

reductions within 24 h of GFP-progerin expression ($p < 0.05$; Fig. 1D). After 1–2 days of GFP-progerin expression the initial drop in all four structural and epigenetic markers stabilized and levels only gradually decreased further over time, all reaching a reduction of approximately 40–50% after 4 days of doxycycline treatment (Figs. 1D, S1). The accumulation of DNA damage markers γH2AX and 53BP1, as measured by a foci-specific detection algorithms (see Section 2), progressed more slowly and reached significance 3 days after induction, after which levels steadily increased (Figs. 1D, S1).

While GFP-lamin A inducible dermal fibroblasts expressed similar levels of induced lamin protein at all time points compared to GFP-progerin fibroblasts (Fig. 1C and D), HGPS characteristic nuclear defects were very modest and significantly different in severity from GFP-progerin induced defects in the case of lamin B1, LAP2, HP1γ, and H3-K27–3M. No activation of DNA damage signaling as measured by γH2AX and 53BP1 foci formation was detected upon induction of GFP-lamin A ($p < 0.05$; Fig. 1D). Preventing farnesylation of progerin by introduction of the C661S mutation fully abolished pathogenic effects of progerin on all tested aging markers (Fig. 1D). These data demonstrate that the GFP-progerin inducible fibroblast cell system recapitulates a wide variety of known HGPS nuclear defects that are progerin specific, depend on progerin's CAAX farnesylation motif and are formed independently of the N-terminal GFP tag within 4 days of GFP-progerin induction. These characteristics make this cell line a suitable tool for application in a high-throughput, high-content screening approach to identify compounds that disrupt early activation of HGPS pro-aging driver pathways.

3.3. A multi-parameter screening assay for HGPS driver pathways

Based on our initial characterization of HGPS defects (Fig. 1D), we designed a multi-parameter screening assay to assess the effect of screened compounds on several HGPS cellular defects simultaneously. Of the structural and epigenetic HGPS markers, lamin B1 changed most robustly (Fig. 1D) and is closely related to progerin in structure and localization and involved in both structural [12] as well as epigenetic regulation [41,45]. The combination of lamin B1 with γH2AX IF staining allows for simultaneous detection of the effect of compounds on early affected HGPS markers like lamin B1 (<2 days of GFP-progerin induction), and late occurring defects in the biologically distinct pathway of DNA damage signaling (>2 days of GFP-progerin induction), in addition to determining the direct impact on protein levels of HGPS-disease causing progerin. Based on these considerations, we selected immunofluorescence co-staining of lamin B1 (640 nm excitation laser/far red) and γH2AX (568 nm/red), together with GFP-progerin (488 nm/-green) as assay read-out parameters. DAPI DNA staining (405 nm/blue) was used to assess cytotoxicity and nuclear segmentation.

3.4. High-content automated quantitative imaging of HGPS aging defects

High-content compound screens require automated quantification of phenotype read-outs in a large number of samples in a single assay. We therefore optimized the use of our GFP-progerin inducible assay in a 384-well plate format on a high-content screening platform consisting of an automated Perkin Elmer Opera spinning-disk confocal microscope, combined with automated quantification of HGPS nuclear defects through customized image

analysis scripts run in the Perkin Elmer Acapella Software environment (Fig. 2A). Optimization of cell plating conditions in 384-well plates, and semi-automated immunofluorescence staining procedures (see Section 2), allowed for the capture of GFP-progerin, lamin B1, γH2AX, and DAPI immunofluorescence signals in at least 300 cells by imaging 10 fields per well in a single focal plane in approximately 40 s (20× objective; Fig. 2B). Customized scripts were generated that allowed for the quantification of all three aging parameters at the single cell level. This involves an initial step where nuclei are segmented based on the DAPI DNA stain, using algorithm parameters with stringency levels that allows for proper segmentation of both well rounded nuclei and classical progerin misshaped nuclei [53] (Fig. 2B), and includes size selection criteria to increase the accuracy of identifying single nuclei (see Section 2). After nuclear segmentation, the average nuclear intensities of both GFP-progerin (Fig. 2C) and lamin B1 (Fig. 2E) were determined on an individual cell basis. Given that γH2AX forms distinct nuclear foci upon activation of DNA damage signaling, we customized our scripts to perform a contrast-based spot detection within the nucleus for γH2AX, and subsequently quantified the number of spots, their intensity and their relative area per cell, combining these 3 parameters into one integrated spot intensity measurement for γH2AX (Fig. 2D). The scripts serve a multi-purpose use as they can be applied to quantification of nuclear intensities of LAP2, HP1γ, and H3-K27–3M aging parameters, as well as for the integrated spot intensity measurements of the DNA damage marker 53BP1, which has a nuclear distribution pattern similar to γH2AX. Taken together, these optimization steps establish an automated high-throughput, high-content imaging pipeline for use in screening of compounds that affect the formation of HGPS aging defects.

3.5. Primary high-throughput screening of FDA-approved small molecules

To provide proof-of-principle that the developed assay can be used to identify compounds that counteract HGPS nuclear defects, we performed a screen of the NPC small molecule library consisting of 2816 FDA-approved compounds [17], using GFP-progerin, lamin B, and γH2AX as the primary HGPS markers (Fig. 3A). Based on our initial observation that a mutation in the farnesylation CAAX motif of progerin renders it incapable of inducing HGPS nuclear defects (Fig. 1D), we used the FTI L-744832 as a positive control. In line with the results for the C661S mutant (Fig. 1D) and the absence of an HGPS disease phenotype in mice expressing similarly mutated progerin [52], we observed that the addition of a single dose of FTI at the time of inducing GFP-progerin fibroblasts was sufficient for the formation of intranuclear progerin foci rather than accumulation at the nuclear periphery, and L-744832 thereby fully prevented the formation of lamin B1 and γH2AX nuclear defects by induced GFP-progerin (Fig. 3B and C). These results demonstrate the importance of progerin farnesylation in HGPS etiology, and suggest that progerin in particular causes HGPS nuclear defects upon farnesylation dependent incorporation into the nuclear lamina. Cells in which GFP-progerin remained uninduced were used as a further positive control (Fig. 3A). Untreated GFP-progerin induced fibroblasts developed a full HGPS phenotype and were used as a negative control (Fig. 3A).

2,816 FDA-approved small molecules were screened at concentrations of 1, 3, 10 and 29 μM in separate 384 well plates by analysis of 300–1000 cells per condition (see Section 2). Z' -scores were calculated based on positive (GFP-progerin induced) and negative controls

(GFP-progerin uninduced) and ranged from 0.17 to 0.83 (see Section 2). After exclusion of compound treatments that reduced cell number by more than two-fold compared to the negative control due to cytotoxic effects, we identified 27 compounds, corresponding to a hit rate of 0.95% (27/2,816), that for at least 2 out of the 4 tested concentrations either significantly reduced GFP-progerin levels (19–29% of effect positive uninduced control), or partially prevented the formation of lamin B1 (82–127%) or γH2AX defects (36–89%; see Section 2; Fig. 3D).

Identified compounds fell into the biologically distinctive categories of corticoids ($N = 11$), phosphodiesterase (PDE) inhibitors ($N = 3$), adrenergic agonists ($N = 3$), retinoids ($N = 2$), and drugs that affect multiple pathways ($N = 8$). Retinoids and corticoids were selected as candidates based on their capability to reduce γH2AX defects and modestly reduce GFP-progerin levels, while also exhibiting drug- and concentration-dependent effects on lamin B1 defects (Figs. 3E, S2A). PDE inhibitors and adrenergic agonists predominantly affected lamin B1 and/or γH2AX without affecting GFP-progerin levels (Fig. S2B). Compounds with various biological effects mostly prevented the formation of lamin B1 defects without affecting GFP-progerin protein levels or γH2AX defects (Fig. S3C). These data provide proof-of-principle that the established HGPS compound screening pipeline enables identification of candidate drugs that show promising effects on reducing the formation of HGPS defects.

3.6. High-content imaging based validation of primary screening candidates in HGPS patient cells

To validate the identified candidate compounds we next tested their effect in HGPS patient cells, thereby confirming our initial screening results in an orthogonal HGPS model system. In addition to lamin B1 and γH2AX defects, we also monitored the effect of each compound on the level of the structural protein LAP2, loss of the epigenetic markers HP1γ and H3-K27–3M, and on DNA damage activated 53BP1, all of which are affected in HGPS patient cells in a progerin-dependent manner [24,33,42] (Fig. 1D). Based on the dose–response curves of the primary screen (Figs. 3D, S2), we tested all 27 positive compounds at a concentration of 10 μM, with the exception of the PDE inhibitor doxofylline, which was shown to be more active at a concentration of 1 μM (Fig. S2B), and further doubled the treatment time to 8 days, based on previous compound testing that showed better effects upon prolonged treatment [7], and on the assumption that it likely takes longer to reverse established aging defects than to prevent their formation in the first place, especially given the particular long half-lives of several of the involved lamin proteins [2]. FTI treatment in HGPS patient cells, and wildtype skin fibroblasts were used as respective positive controls for all aging defects (Fig. 4), with the exception of endogenous progerin protein levels and lamin B1 defects which were not changed in HGPS patient cells by FTI treatment as previously reported [1]. While we did not observe any significant improvement for HGPS aging defects upon treatment with corticoid compounds or drugs with various biological effects, we did monitor a modest effect of the adrenergic agonists salbutamol sulfate (compound #8, Fig. 4), and the PDE inhibitor milrinone (compound #3) on increasing HP1γ levels (+18–20%, $p < 0.05$, Fig. 4). In addition, the adrenergic agonist procaterol hydrochloride hemihydrate slightly increased H3-K27–3M levels (+15%; compound #7; $p <$

0.05; Fig. 4). However, both retinoids tretinoin and tazarotene showed strong and significant effects on all tested aging parameters (Fig. 4). Treatment with retinoids, lowered progerin levels by approximately two-fold and reduced DNA damage effects as measured by γH2AX and 53BP1 foci formation by about 50% (Fig. 4). Lamin B1 levels were restored to levels comparable to wildtype fibroblasts and the HGPS characteristic reduction in LAP2, HP1γ, and H3-K27–3M markers was restored to levels 20–60% higher than measured in wildtype control cells (Fig. 4). These data demonstrate that the GFP-progerin inducible cell assay can be used to identify novel classes of compounds that can both prevent formation of HGPS aging defects as well as reverse established aging defects in HGPS patient cells.

3.7. Clinically used retinoids lower expression of A-type lamins and rescue HGPS aging defects

Given the robust rescue of the HGPS phenotype by retinoids identified in our screen, we further explored their mode of action and therapeutic potential by performing dose–response studies on three biologically distinct, clinically-used, and well-tolerated retinoids isotretinoin, tamibarotene and tazarotene. FDA approved isotretinoin, also known as 13-cis retinoic acid, is primarily used in oral form as a treatment for cystic acne that is irresponsive to topical retinoids like tretinoin, and is converted into active metabolites that act as agonists of the retinoic acid receptors (RAR) α, β, and γ as well as the retinoid X receptors (RXR) [29]. Tamibarotene (AM80) is currently marketed in Japan for treatment of acute promyelocytic leukemia (APL) and is a RAR agonist with high specificity for RARα and β over RARγ [28]. Tazarotene is currently only FDA approved for topical use in treatment of psoriasis and cystic acne by selectively activating RARβ and γ nuclear receptors, but clinically favorable effects have been shown as well for oral forms [50].

Treating HGPS patient cells with either of these RAR agonists demonstrated that all three retinoids were equally capable of lowering progerin levels by two-fold and restoring lamin B1, LAP2, HP1γ, and H3-K27–3M defects fully while reducing DNA damage markers γH2AX and 53BP1 by ~50% (Figs. 5A, S3). Part of these effects were reached by treatment in the low nanomolar range. For example treatment at 100 nM of all three retinoids fully restored H3-K27–3M defects and HP1c defects were partially rescued at concentrations as low as 1–10 nM of isotretinoin and tazarotene (Fig. S3). In contrast, the pan-RAR antagonist BMS493 [8] worsened aging defects in HGPS patient cells. BMS493 slightly increased progerin levels by 24%, and further decreased protein levels of lamin B1 (−15%), LAP2 (−38%), HP1γ (−47%), and H3-K27–3M (−25%) without significantly increasing DNA damage markers (Fig. S3). This suggests that retinoids exert their protective effects through activation of RAR receptors, most likely through a global down-regulation of not only progerin, but also lamin A and C at the protein and mRNA level (Fig. 5A and B), without affecting the ratios between lamin A, C and progerin (Fig. S4). This is in line with a recent report that identified RAR regulatory elements in the *LMNA* promoter as a biological mechanism to reduce the activity of the *LMNA* promoter thereby fine-tuning global expression levels of A-type lamins [47]. In conclusion, we demonstrate the development of a GFP-progerin inducible assay and provide proof-of-principle of its use in a high-throughput imaging screen by identifying retinoids as potential anti-progeric agents.

4. Discussion

HGPS is a lethal premature aging disease caused by the dominant-negative acting lamin A mutant progerin, which causes extensive defects in structural, epigenetic, and DNA damage signaling cellular pathways [14]. While recent research efforts have described deregulations in key modulators of various cellular processes in HGPS patient cells, it is unclear whether these are causative or merely secondary bystander effects of HGPS etiology, especially given the fact that most affected pathways are interconnected [5,33,37]. Using HGPS patient cells as a primary resource for identification of druggable targets in cellular pathways that drive HGPS formation is challenging for this reason. While such approaches have been successful in the identification of a select few druggable targets that help alleviate HGPS symptoms, particularly farnesyl transferases and mTOR [7,53], there is an urgent need for complementary methodologies that allow for the identification of druggable HGPS-driving targets in a high-throughput unbiased manner.

To this end, we report here the development of a progerin-inducible system in a wildtype fibroblast background that allows monitoring the formation of HGPS characteristic defects by progerin over time, thereby aiding in distinguishing immediate early defects which are more likely to drive HGPS formation, from later occurring downstream bystander defects. A similar system, but using a doxycycline repressed (tet-off) promoter led to the discovery that a decrease in the heterochromatin promoting proteins Rbbp4 and Rbbp7 by progerin precedes and contributes to the activation of DNA damage signaling [33], demonstrating the ability to extract mechanistic data based on observation of the temporal sequence of HGPS defects. A disadvantage of tet-off models is that they take longer to induce proteins due to the fact that doxycycline binds to the extracellular matrix and therefore cannot be immediately washed away to induce expression of the target protein [38]. Furthermore the reproducibility of tet-off systems in inducing HGPS defects is expected to be lower based on the fact that it is more difficult to reproducibly wash out doxycycline than to add it in a tet-on setting, which is important for high-throughput assays were reproducibility is key. We therefore generated a GFP-progerin inducible wildtype fibroblast cell line, using a lentiviral third generation tet-on inducible system based on the tetracycline repressor A3 mutant [6]. This system is characterized by nearly undetectable progerin levels under regular growth conditions and steadily induced GFP-progerin to levels comparable to endogenous lamin A in the presence of doxycycline, establishing HGPS defects as early as 12 h after the start of induction as compared to 3–4 days for tet-off GFP-progerin fibroblasts [44]. This system is also advantageous for large scale screening applications since it does not require the use of expensive doxycycline-free FBS in the culture medium. HGPS defects occurred in a similar order as previously reported [33], in that heterochromatic defects became apparent before the activation of DNA damage signaling pathways. These HGPS defects were, furthermore, specific to progerin and independent of the N-terminal GFP tag as indicated by the fact that both GFP-lamin A and the farnesylation mutant GFP-progerin C661S were unable to recapitulate GFP-progerin induced aging effects for various structural, epigenetic, and DNA damaging markers previously reported to occur in HGPS patient cells [43].

The short timeframe for the induction of a full HGPS phenotype in the established inducible system allows for direct screening of anti-progeroid effects of compounds in a 384-well

plate format, because GFP-progerin inducible fibroblasts can simultaneously be plated and induced for GFP-progerin expression in the presence and absence of compounds without the necessity to replace compounds or trypsinize cells during the assay. The ability to store fixed cells long-term provides users with the flexibility of testing large compound libraries in several batches before proceeding with semi-automated fluorescent staining, or alternatively perform immunofluorescence (IF) staining on accumulated 384-well assay plates in batches before proceeding with imaging and quantification of the aging defects. The use of IF staining further provides the opportunity to tailor the assay for specific aging endpoints if needed, which can be readily quantified with established detection algorithms. While we chose to use progerin, lamin B1, and γH2AX as the endpoints for our primary high-throughput screen, based on the fact that they changed robustly and represent biologically distinct HGPS affected pathways, we broadened our assay to a panel of 4 more HGPS markers (LAP2, HP1γ, H3-K27–3M and 53BP1) in validation experiments of lead candidate compounds from our primary screen, to further test their capability to globally ameliorate HGPS defects in HGPS patient cells.

The ability to screen for multiple aging markers in a single assay allows for more stringent hit selection as demonstrated by a hit rate of ~1% in our primary screen. To further increase the stringency of the high-throughput HGPS drug discovery pipeline we chose to validate the 27 candidate compounds in primary HGPS patient cells to identify compounds that not only were capable of preventing the formation of progerin-induced nuclear defects, but are also effective in reversing already established aging defects in HGPS patient cells. This resulted in the identification of 2 retinoids, tretinoin and tazarotene, that reversed all tested aging defects in HGPS patient cells. The follow-up experiments on isotretinoin, tamibarotene, and tazarotene, which all have clinically favorable biosafety profiles in treatment of acne, psoriasis, or APL over other oral retinoids [29,50], indicate that retinoids have anti-progeroid effects through lowering expression of A-type lamins in a RAR-dependent manner. These observations are in line with the finding that retinoid bound RARs bind to a retinoic acid receptor element (RARE) in the *LMNA* promoter, thereby repressing lamin A, progerin and lamin C expression at the mRNA level [47]. It remains to be determined in follow-up animal studies whether retinoid-induced reduction of endogenous lamin A and C protein levels might have a potential negative impact on physiological processes, such as differentiation, that are linked to lamin A/C expression [9]. In that regard, previous observations showing that lamin A appears dispensable in mouse models that express lamin C only [11], as well as the observation that *LMNA* haploinsufficiency does not have any overt physiological impact [19,46], and that eliminating expression of endogenous lamin A in a progerin expressing mouse model helps alleviate the HGPS disease phenotype [54], encourage follow-up studies in mouse models to further determine the efficacy and mechanisms through which retinoids may counteract HGPS aging defects. Besides directly lowering progerin expression, retinoids likely have additional anti-progeroid effects based on our observation that they can prevent the formation of HGPS aging defects in our GFP-progerin inducible cell model where progerin expression is driven by a doxycycline responsive promoter and not the endogenous *LMNA* promoter, and therefore unaffected by retinoids. A possible mode of action of retinoids in the progerin-inducible cell line is suggested by the finding that the HGPS disease phenotype of mice that express

progerin is ameliorated by eliminating the expression of endogenous lamin A to reduce total A-type lamin levels [54]. It is thus possible that retinoids partially prevent the formation of lamin B1 and γH2AX defects by GFP-progerin in the inducible system through lowering endogenous lamin A and C levels, while leaving GFP-progerin levels mostly unaltered. This further indicates that our assay, despite the use of an inducible promoter, is suitable to detect anti-progeroid compounds that modulate the *LMNA* promoter.

Although we cannot formerly rule out that minor technical and biological differences between progerin-inducible and HGPS patient cell lines could result in the detection of false positive candidates, overall the combination of multiple read-outs and the use of two independent assays for the primary and validation screen adds considerable stringency to the final hit selection. We further recommend the pairing of both assays as this provides an independent verification of any discovered hits, and helps the overall identification of HGPS disease relevant pathways that might be missed by only using one method. For example, FTI's are known to not reverse DNA damage once it has been established in HGPS patient cells [25]. By using the inducible system we now find that blocking farnesylation of the C terminal tail of progerin, by either mutating the CAAX motif or by FTI treatment, prevents the formation of DNA damage. These finding are in line with a proposed HGPS disease model [30] where DNA damage is reversible during early stages, but becomes irreversible in later phases due to secondary effects, like the sequestration of the XPA protein.

Our screen identified several compounds which are able to reverse already established aging defects in HGPS patient cells. In addition, several compound classes, including PDE inhibitors, adrenergic agonists and corticoids, were identified which are involved in the activation of cellular signaling pathways that are capable of preventing the formation of aging defects by progerin although they are unable to reverse established defects in the presence of progerin. While these compounds are unlikely to have direct clinical use in HGPS, their use may be informative in identifying cellular targets in HGPS relevant pathways that are directly affected by progerin. For example, B-adrenergic receptor agonists and PDE inhibitors are known to increase cellular cAMP (cyclic adenosine monophosphate) levels by increasing its synthesis from ATP and inhibiting its conversion into 5′ -AMP respectively, which results in downstream activation of AMPK and PCG1α in a SIRT1 dependent manner [13,36]. AMPK and PCG1α activation have both been hypothesized to alleviate HGPS symptoms [10,27], and SIRT1 deacetylase activity, which is required for their activation is directly inhibited by progerin [23]. Potential anti-progeroid effects of PDE inhibitors and adrenergic agonists on the cAMP-SIRT1-AMPK-PCG1α pathway would therefore only be picked up in the inducible system, where the activity of this pathway can be increased before progerin abrogates SIRT1 functioning, while the treatment would be ineffective in HGPS patient cells in which SIRT1 is already impaired. The validity of using these hits to identify novel drug targets is indicated by the fact that the SIRT1 activator resveratrol has been shown to alleviate HGPS symptoms [23]. The recently reported role of resveratrol in activating SIRT1 directly, as well as indirectly through inhibiting PDEs [32], further strengthens the notion that the identification of PDE inhibitors in our primary screen is likely not an artifact. A similar unknown mechanism might be at work for corticoid signaling, given that glucocorticoids have been reported to inhibit senescence-associated

secretory phenotypes in part by suppressing NFkB inflammatory responses [21], which are an important component of HGPS etiology [31].

In conclusion, we have here established a novel method that strengthens our capabilities of high-throughput, high-content, imaging based identification of anti-progeroid compounds. The adaptability of the GFP-progerin inducible assay system also provides opportunities to further investigate the relevance and mechanistic details of candidate HGPS pathways, not only by investigating compounds that activate these pathways, but also by its combined use with complementary assay such as fluorescent or bioluminescent reporters, targeted RNAi mediated knockdowns, or virally transduced overexpression of key regulators within such pathways. We anticipate that the availability of a phenotype-based assay for HGPS discovery will catalyze efforts in the HGPS community to further define the molecular mechanisms of HGPS driver pathways and to discover novel HGPS drugs.

Supplementary Material

Refer to Web version on PubMed Central for supplementary material.

Acknowledgements

We thank members of the Misteli lab for providing helpful feedback and experimental suggestions. This research was supported by the Intramural Research Program of the National Institutes of Health (NIH), NCI, Center for Cancer Research and by a grant for the Progeria Research Foundation.

References

[1]. Adam SA, Butin-Israeli V, Cleland MM, Shimi T, Goldman RD, Disruption of lamin B1 and lamin B2 processing and localization by farnesyltransferase inhibitors, Nucleus 4 (2013) 142–150. [PubMed: 23475125]

[2]. Boisvert FM, Ahmad Y, Gierlinski M, Charriere F, Lamont D, Scott M, Barton G, Lamond AI, A quantitative spatial proteomics analysis of proteome turnover in human cells, Mol. Cell. Proteomics: MCP 11 (M111) (2012) 011429. [PubMed: 21937730]

[3]. Bosch-Presegue L, Raurell-Vila H, Marazuela-Duque A, Kane-Goldsmith N, Valle A, Oliver J, Serrano L, Vaquero A, Stabilization of Suv39H1 by SirT1 is part of oxidative stress response and ensures genome protection, Mol. Cell 42 (2011) 210–223. [PubMed: 21504832]

[4]. Broers JL, Hutchison CJ, Ramaekers FC, Laminopathies J Pathol. 204 (2004) 478–488.

[5]. Burtner CR, Kennedy BK, Progeria syndromes and ageing: what is the connection?, Nat Rev. Mol. Cell Biol 11 (2010) 567–578. [PubMed: 20651707]

[6]. Campeau E, Ruhl VE, Rodier F, Smith CL, Rahmberg BL, Fuss JO, Campisi J, Yaswen P, Cooper PK, Kaufman PD, A versatile viral system for expression and depletion of proteins in mammalian cells, PLoS One 4 (2009) e6529. [PubMed: 19657394]

[7]. Cao K, Graziotto JJ, Blair CD, Mazzulli JR, Erdos MR, Krainc D, Collins FS, Rapamycin reverses cellular phenotypes and enhances mutant protein clearance in Hutchinson–Gilford progeria syndrome cells, Sci. Transl. Med 3 (2011) 89ra58.

[8]. Das BC, Tang XY, Evans T, Design and synthesis of boron containing potential pan-RAR inverse agonists, Tetrahedron Lett. 53 (2012) 1316–1318. [PubMed: 23180890]

[9]. Dittmer TA, Sahni N, Kubben N, Hill DE, Vidal M, Burgess RC, Roukos V, Misteli T, Systematic identification of pathological lamin A interactors, Mol. Biol. Cell 25 (2014) 1493–1510. [PubMed: 24623722]

[10]. Finley J, Alteration of splice site selection in the LMNA gene and inhibition of progerin production via AMPK activation, Med. Hypotheses 83 (2014) 580–587. [PubMed: 25216752]

[11]. Fong LG, Ng JK, Lammerding J, Vickers TA, Meta M, Cote N, Gavino B, Qiao X, Chang SY, Young SR, et al., Prelamin A and lamin A appear to be dispensable in the nuclear lamina, J. Clin. Invest 116 (2006) 743–752. [PubMed: 16511604]

[12]. Funkhouser CM, Sknepnek R, Shimi T, Goldman AE, Goldman RD, Olvera de la Cruz M, Mechanical model of blebbing in nuclear lamin meshworks, Proc. Natl. Acad. Sci. U.S.A 110 (2013) 3248–3253. [PubMed: 23401537]

[13]. Gerhart-Hines Z, Dominy JE, Jr., Blattler SM, Jedrychowski MP, Banks AS, Lim JH, Chim H, Gygi SP, Puigserver P, The cAMP/PKA pathway rapidly activates SIRT1 to promote fatty acid oxidation independently of changes in NAD(+), Mol. Cell 44 (2011) 851–863. [PubMed: 22195961]

[14]. Gonzalez JM, Pla D, Perez-Sala D, Andres V, A-type lamins and Hutchinson–Gilford progeria syndrome: pathogenesis and therapy, Front. Biosci. (Scholar Ed.) 3 (2011) 1133–1146.

[15]. Gordon LB, Kleinman ME, Miller DT, Neuberg DS, Giobbie-Hurder A, Gerhard-Herman M, Smoot LB, Gordon CM, Cleveland R, Snyder BD, et al., Clinical trial of a farnesyltransferase inhibitor in children with Hutchinson–Gilford progeria syndrome, Proc. Natl. Acad. Sci. U.S.A 109 (2012) 16666–16671. [PubMed: 23012407]

[16]. Gordon LB, Rothman FG, Lopez-Otin C, Misteli T, Progeria: a paradigm for translational medicine, Cell 156 (2014) 400–407. [PubMed: 24485450]

[17]. Huang R, Southall N, Wang Y, Yasgar A, Shinn P, Jadhav A, Nguyen DT, Austin CP, The NCGC pharmaceutical collection: a comprehensive resource of clinically approved drugs enabling repurposing and chemical genomics, Sci. Transl. Med 3 (2011) 80ps16.

[18]. Kubben N, Adriaens M, Meuleman W, Voncken JW, van Steensel B, Misteli T, Mapping of lamin A- and progerin-interacting genome regions, Chromosoma 121 (2012) 447–464. [PubMed: 22610065]

[19]. Kubben N, Voncken JW, Konings G, van Weeghel M, van den Hoogenhof MM, Gijbels M, van Erk A, Schoonderwoerd K, van den Bosch B, Dahlmans V, et al., Post-natal myogenic and adipogenic developmental: defects and metabolic impairment upon loss of A-type lamins, Nucleus 2 (2011) 195–207. [PubMed: 21818413]

[20]. Kudlow BA, Kennedy BK, Monnat RJ, Jr., Werner and Hutchinson–Gilford progeria syndromes: mechanistic basis of human progeroid diseases, Nat. Rev. Mol. Cell Biol. 8 (2007) 394–404. [PubMed: 17450177]

[21]. Laberge RM, Zhou L, Sarantos MR, Rodier F, Freund A, de Keizer PL, Liu S, Demaria M, Cong YS, Kapahi P, et al., Glucocorticoids suppress selected components of the senescence-associated secretory phenotype, Aging Cell 11 (2012) 569–578. [PubMed: 22404905]

[22]. Larrieu D, Britton S, Demir M, Rodriguez R, Jackson SP, Chemical inhibition of NAT10 corrects defects of laminopathic cells, Science 344 (2014) 527–532. [PubMed: 24786082]

[23]. Liu B, Ghosh S, Yang X, Zheng H, Liu X, Wang Z, Jin G, Zheng B, Kennedy BK, Suh Y, et al., Resveratrol rescues SIRT1-dependent adult stem cell decline and alleviates progeroid features in laminopathy-based progeria, Cell Metab. 16 (2012) 738–750. [PubMed: 23217256]

[24]. Liu B, Wang Z, Zhang L, Ghosh S, Zheng H, Zhou Z, Depleting the methyltransferase Suv39h1 improves DNA repair and extends lifespan in a progeria mouse model, Nat. Commun 4 (2013) 1868. [PubMed: 23695662]

[25]. Liu Y, Rusinol A, Sinensky M, Wang Y, Zou Y, DNA damage responses in progeroid syndromes arise from defective maturation of prelamin A, J. Cell Sci 119 (2006) 4644–4649. [PubMed: 17062639]

[26]. Liu Y, Wang Y, Rusinol AE, Sinensky MS, Liu J, Shell SM, Zou Y, Involvement of xeroderma pigmentosum group A (XPA) in progeria arising from defective maturation of prelamin A, FASEB J. 22 (2008) 603–611. [PubMed: 17848622]

[27]. Lopez-Mejia IC, de Toledo M, Chavey C, Lapasset L, Cavelier P, Lopez-Herrera C, Chebli K, Fort P, Beranger G, Fajas L, et al., Antagonistic functions of LMNA isoforms in energy expenditure and lifespan, EMBO Rep. 15 (2014) 529–539. [PubMed: 24639560]

[28]. Miwako I, Kagechika H, Tamibarotene, Drugs Today 43 (2007) 563–568 (Barcelona, Spain: 1998). [PubMed: 17925887]

[29]. Moise AR, Pharmacology of Retinoid Receptors, Tocris Biosci. Sci. Rev. Ser (2014) 1–12.

[30]. Musich PR, Zou Y, Genomic instability and DNA damage responses in progeria arising from defective maturation of prelamin A, Aging 1 (2009) 28–37. [PubMed: 19851476]

[31]. Osorio FG, Barcena C, Soria-Valles C, Ramsay AJ, de Carlos F, Cobo J, Fueyo A, Freije JM, Lopez-Otin C, Nuclear lamina defects cause ATM-dependent NF-kappaB activation and link accelerated aging to a systemic inflammatory response, Genes Dev. 26 (2012) 2311–2324. [PubMed: 23019125]

[32]. Park SJ, Ahmad F, Philp A, Baar K, Williams T, Luo H, Ke H, Rehmann H, Taussig R, Brown AL, et al., Resveratrol ameliorates aging-related metabolic phenotypes by inhibiting cAMP phosphodiesterases, Cell 148 (2012) 421–433. [PubMed: 22304913]

[33]. Pegoraro G, Kubben N, Wickert U, Gohler H, Hoffmann K, Misteli T, Ageing-related chromatin defects through loss of the NURD complex, Nat. Cell Biol 11 (2009) 1261–1267. [PubMed: 19734887]

[34]. Pegoraro G, Voss TC, Martin SE, Tuzmen P, Guha R, Misteli T, Identification of mammalian protein quality control factors by high-throughput cellular imaging, PLoS One 7 (2012) e31684. [PubMed: 22363705]

[35]. Pelz O, Gilsdorf M, Boutros M, Web cellHTS2: a web-application for the analysis of high-throughput screening data, BMC Bioinf. 11 (2010) 185.

[36]. Price NL, Gomes AP, Ling AJ, Duarte FV, Martin-Montalvo A, North BJ, Agarwal B, Ye L, Ramadori G, Teodoro JS, et al., SIRT1 is required for AMPK activation and the beneficial effects of resveratrol on mitochondrial function, Cell Metab. 15 (2012) 675–690. [PubMed: 22560220]

[37]. Prokocimer M, Barkan R, Gruenbaum Y, Hutchinson–Gilford progeria syndrome through the lens of transcription, Aging Cell 12 (2013) 533–543. [PubMed: 23496208]

[38]. Rennel E, Gerwins P, How to make tetracycline-regulated transgene expression go on and off, Anal. Biochem 309 (2002) 79–84. [PubMed: 12381365]

[39]. Richards SA, Muter J, Ritchie P, Lattanzi G, Hutchison CJ, The accumulation of un-repairable DNA damage in laminopathy progeria fibroblasts is caused by ROS generation and is prevented by treatment with N-acetyl cysteine, Hum. Mol. Genet 20 (2011) 3997–4004. [PubMed: 21807766]

[40]. Roukos V, Voss TC, Schmidt CK, Lee S, Wangsa D, Misteli T, Spatial dynamics of chromosome translocations in living cells, Science 341 (2013) 660–664. [PubMed: 23929981]

[41]. Sadaie M, Salama R, Carroll T, Tomimatsu K, Chandra T, Young AR, Narita M, Perez-Mancera PA, Bennett DC, Chong H, et al., Redistribution of the Lamin B1 genomic binding profile affects rearrangement of heterochromatic domains and SAHF formation during senescence, Genes Dev. 27 (2013) 1800–1808. [PubMed: 23964094]

[42]. Scaffidi P, Misteli T, Reversal of the cellular phenotype in the premature aging disease Hutchinson–Gilford progeria syndrome, Nat. Med 11 (2005) 440–445. [PubMed: 15750600]

[43]. Scaffidi P, Misteli T, Lamin A-dependent nuclear defects in human aging, Science 312 (2006) 1059–1063. [PubMed: 16645051]

[44]. Scaffidi P, Misteli T, Lamin A-dependent misregulation of adult stem cells associated with accelerated ageing, Nat. Cell Biol 10 (2008) 452–459. [PubMed: 18311132]

[45]. Shah PP, Donahue G, Otte GL, Capell BC, Nelson DM, Cao K, Aggarwala V, Cruickshanks HA, Rai TS, McBryan T, et al., Lamin B1 depletion in senescent cells triggers large-scale changes in gene expression and the chromatin landscape, Genes Dev. 27 (2013) 1787–1799. [PubMed: 23934658]

[46]. Sullivan T, Escalante-Alcalde D, Bhatt H, Anver M, Bhat N, Nagashima K, Stewart CL, Burke B, Loss of A-type lamin expression compromises nuclear envelope integrity leading to muscular dystrophy, J. Cell Biol 147 (1999) 913–920. [PubMed: 10579712]

[47]. Swift J, Ivanovska IL, Buxboim A, Harada T, Dingal PC, Pinter J, Pajerowski JD, Spinler KR, Shin JW, Tewari M, et al., Nuclear lamin-A scales with tissue stiffness and enhances matrix-directed differentiation, Science 341 (2013) 1240104. [PubMed: 23990565]

[48]. Toth JI, Yang SH, Qiao X, Beigneux AP, Gelb MH, Moulson CL, Miner JH, Young SG, Fong LG, Blocking protein farnesyltransferase improves nuclear shape in fibroblasts from humans with progeroid syndromes, Proc. Natl. Acad. Sci. U.S.A 102 (2005) 12873–12878. [PubMed: 16129834]

[49]. Villa-Bellosta R, Rivera-Torres J, Osorio FG, Acin-Perez R, Enriquez JA, Lopez-Otin C, Andres V, Defective extracellular pyrophosphate metabolism promotes vascular calcification in a mouse model of Hutchinson–Gilford progeria syndrome that is ameliorated on pyrophosphate treatment, Circulation 127 (2013) 2442–2451. [PubMed: 23690466]

[50]. Walker PS, Tazarotene in the treatment of psoriasis FDA advisory committee meeting. <http://www.fda.gov/ohrms/dockets/ac/04/slides/2004-4062S1_02_Allergan-Presentation.ppt>, 2004.

[51]. Wang RH, Sengupta K, Li C, Kim HS, Cao L, Xiao C, Kim S, Xu X, Zheng Y, Chilton B, et al., Impaired DNA damage response, genome instability, and tumorigenesis in SIRT1 mutant mice, Cancer Cell 14 (2008) 312–323. [PubMed: 18835033]

[52]. Yang SH, Chang SY, Ren S, Wang Y, Andres DA, Spielmann HP, Fong LG, Young SG, Absence of progeria-like disease phenotypes in knock-in mice expressing a non-farnesylated version of progerin, Hum. Mol. Genet 20 (2011) 436–444. [PubMed: 21088111]

[53]. Yang SH, Meta M, Qiao X, Frost D, Bauch J, Coffinier C, Majumdar S, Bergo MO, Young SG, Fong LG, A farnesyltransferase inhibitor improves disease phenotypes in mice with a Hutchinson–Gilford progeria syndrome mutation, J. Clin. Invest 116 (2006) 2115–2121. [PubMed: 16862216]

[54]. Yang SH, Qiao X, Farber E, Chang SY, Fong LG, Young SG, Eliminating the synthesis of mature lamin A reduces disease phenotypes in mice carrying a Hutchinson–Gilford progeria syndrome allele, J. Biol. Chem 283 (2008) 7094–7099. [PubMed: 18178963]

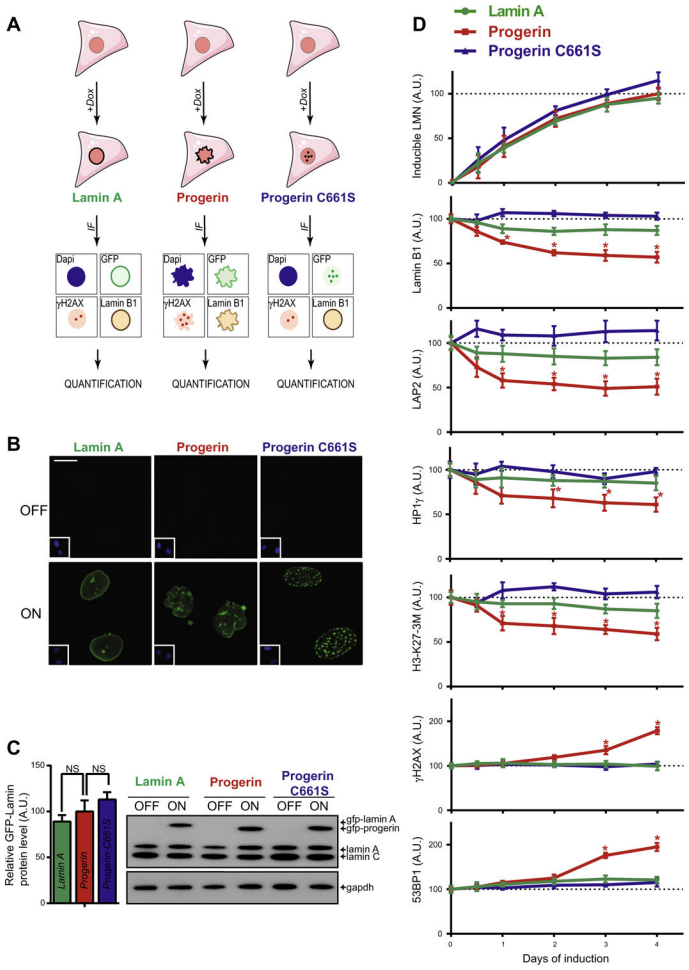

Fig. 1.

Characterization of an inducible GFP-progerin fibroblast cell system. (A) Schematic representation of stable human dermal fibroblasts cell lines containing doxycycline-inducible GFP-tagged lamin A, progerin or progerin C661S mutant for use in immunofluorescence (IF) detection of GFP, lamin B1, γH2AX, and DNA DAPI stain. (B) Representative IF images of DNA DAPI stain (inset bottom left) and GFP signal of all three GFP-lamin inducible fibroblasts cell lines in the absence and presence of doxycycline for 4 days. Scale bar: 10 μM. (C) Western blot for uninduced and 4 days induced GFP-lamin fibroblast cell lines and quantification of β-actin normalized lamin protein levels. Values represent averages ± SD from 3 experiments. ($p > 0.05$). (D) Quantification of IF signals (see Section 2) of induced GFP-lamin protein levels as well as lamin B1, LAP2, HP1γ, tri-methylated lysine 27 on histone 3 (H3-K27–3M), γH2AX and 53BP1 HGPS markers. Values represent averages ± SD from 3 experiments ($N > 300$, $^*p < 0.05$ between GFP-lamin A and GFP-progerin cell lines).

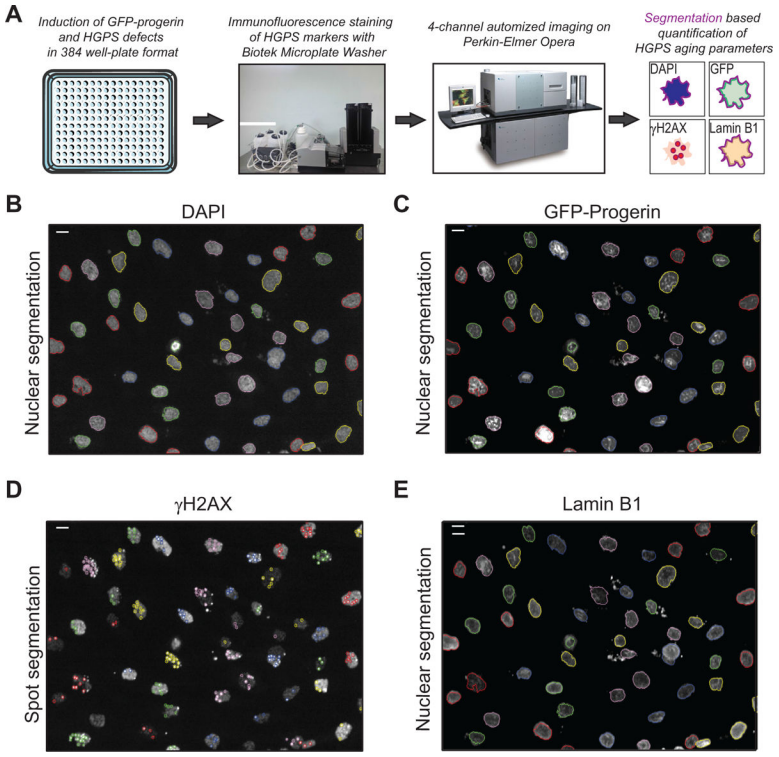

Fig. 2.

High-content imaging quantification of HGPS defects. (A) Schematic representation of the pipeline used for automated detection and quantification of HGPS defects in GFP-progerin inducible fibroblasts. (B, C, E) Representative image of nuclear segmentation based on the DNA DAPI signal in GFP-progerin inducible fibroblasts (4 days, 1 μg/ml doxycycline), shown for DAPI stain (A), GFP-progerin (B) and lamin B1 IF staining (D); scale bar: 10 μM. (D) Example of contrast-based segmentation of γH2AX foci in GFP-progerin inducible fibroblasts (4 days, 1 μg/ml doxycycline). Scale bar: 10 μM.

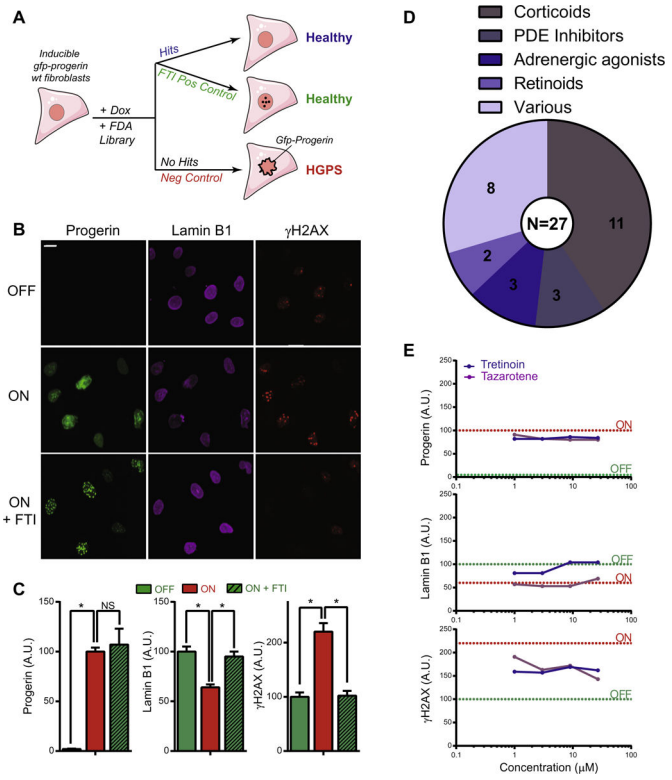

Fig. 3.

High-throughput screening of FDA-approved compound library in GFP-progerin inducible fibroblasts. (A) Overview of the screening assay. GFP-progerin inducible fibroblasts are plated in the presence of doxycycline and treated at the same time with FDA approved compounds that either have no effect on the induction of GFP-progerin and formation of lamin B1 and γH2AX HGPS aging defects (no hits), or alternatively are considered hits based on improving any of these endpoints. Untreated, induced GFP-progerin cells served as negative controls and positive controls are cells in which GFP-progerin remains either uninduced or is induced in the presence of FTI (see Section 2). (B) Immunofluorescence images of positive and negative controls for all assay endpoints. Scale bar: 10 μM. (C) Quantification (see Section 2) of panel B. $N > 300$; $*p < 0.05$. Values represent averages ± SD from 3 experiments. (D) Hit selection of candidate compounds identified from the screen and the respective biological classes they fall in. (E) Dose–response curves from screen identified retinoid compounds (tretinoin, and isotretinoin) based on the effect at 1, 3, 10, and 29 μM concentrations on the induction of GFP-progerin and on lamin B1 and γH2AX markers. Positive and negative control levels for all aging markers are indicated by dotted lines in green and red, respectively. Values represent averages ± SD from 3 experiments.

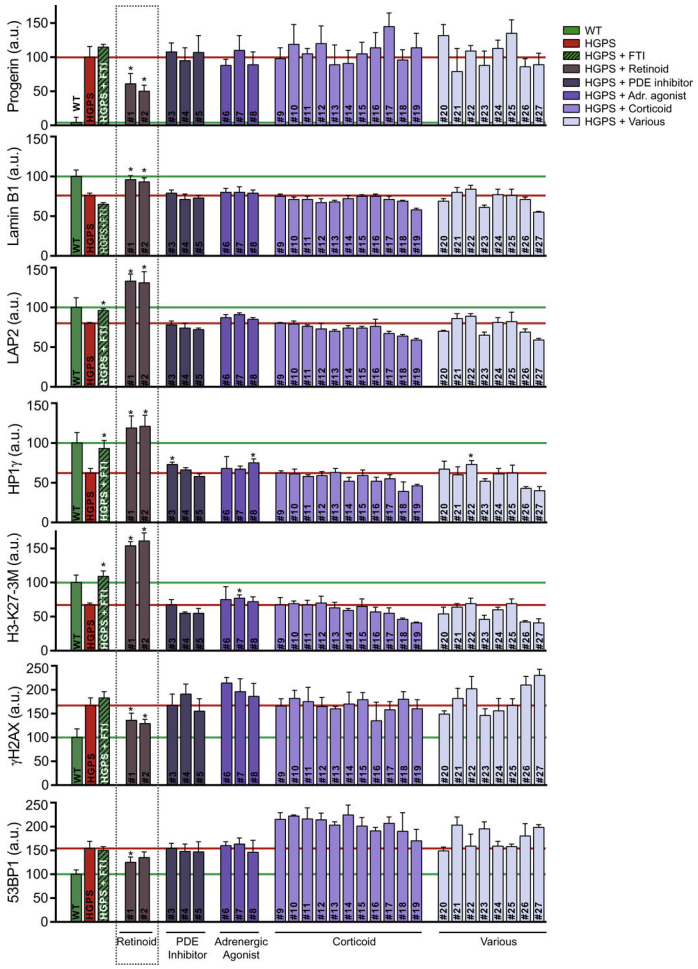

Fig. 4.

Validation screen of FDA-approved candidate compounds in HGPS patient fibroblasts. Quantitative analysis of immunofluorescence staining (see Section 2) for progerin, lamin B1, LAP2, HP1γ, H3-K273M, γH2AX and 53BP1 HGPS markers in HGPS patient fibroblasts that were treated for 8 days with candidate compounds identified in the primary screen. A dose of 10 μM compounds was used for each compound with the exception of doxofylline (1 μM), based on primary screening results. Values represent averages ± SD from 3 experiments. $N > 300$; $*p < 0.05$, untreated HGPS vs. compound treated HGPS. Compounds: #1, tretinoin; #2, tazarotene; #3, milrinone; #4, trequinsin hydrochloride; #5, doxofylline; #6, isoproterenol hydrochloride; #7, procaterol hydrochloride hemihydrates; #8, salbutamol sulfate; #9, hydrocortisone succinate; #10, deflazacort; #11, triamcinolone acetonide; #12, loteprednoletabonate; #13, resocortol butyrate; #14, diflucortolone valerate; #15, betapar; #16, prednisolone acetate; #17, diflorasonediacetate; #18, rimexolone; #19, fludrocortisones acetate; #20, 3,4-dihydroxy-2-(methylamino)acetophenone hydrochloride; #21, sumatriptan succinate; #22, cisplatin; #23, mozavaptan; #24, 2-ethylhexyl salicylate; #25, sulfacetamide; #26, benzethonium chloride; #27, albendazole.

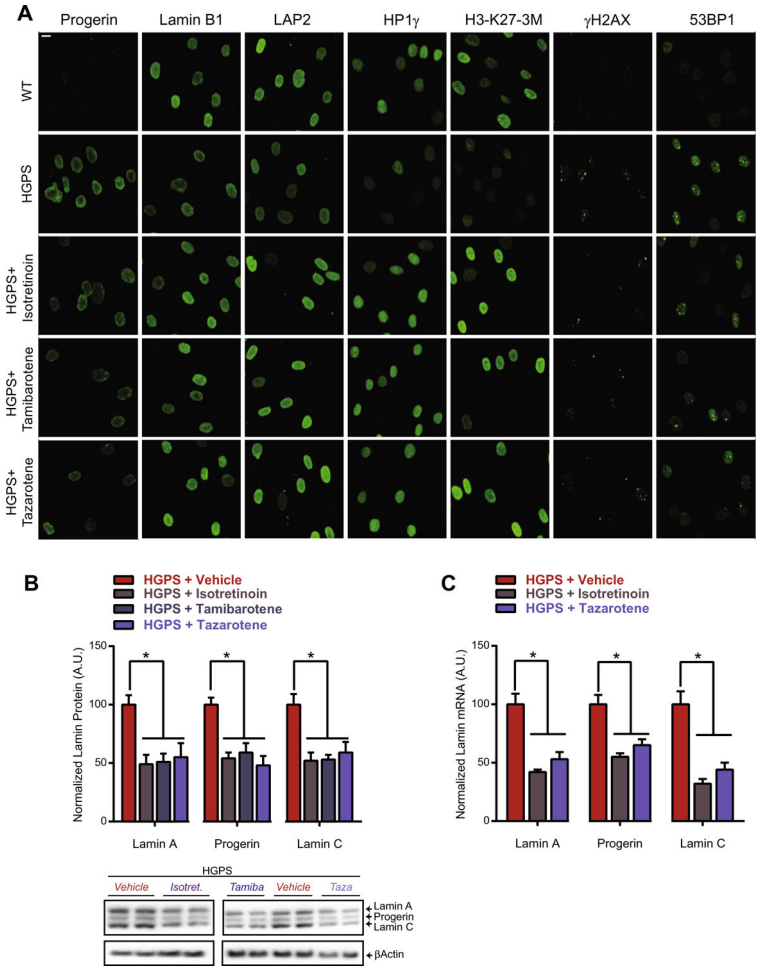

Fig. 5.

Retinoids reduce the expression of A-type lamins and reverse aging defects in HGPS patient fibroblasts. (A) Representative immunofluorescence images of indicated HGPS markers in HGPS patient and wildtype fibroblasts treated with 10 lM of isotretinoin, tamibarotene, or tazarotene. Scale bar: 10 μM. (B) Western blot and quantification of the effect of all three retinoids on the protein levels of A-type lamins in HGPS patient fibroblasts. Values represent averages ± SD from 3 experiments. *$p < 0.05$ treated vs. untreated HGPS patient fibroblasts. (C) Expression analysis of lamin A, progerin and lamin C mRNA levels normalized for GAPDH mRNA expression in HGPS patient fibroblasts upon treatment with 10 μM of isotretinoin or tazarotene. Values represent averages ± SD from 3 experiments. *$p < 0.05$ treated vs. untreated HGPS patient fibroblasts.